encit 2020

ABCM Associação Brasileira de Engenharia e Ciências Mecânicas

18th Brazilian Congress of Thermal Sciences and Engineering
November 16-20, 2020 (Online)

ENCIT2020-0131
EXERGY AND EXERGOENVIRONMENTAL ANALYSES OF A SPARK-IGNITION ENGINE

Daniel R. S. da Silva
Federal University of Rio Grande do Norte, Department of Mechanical Engineering, 59072-970, Natal/RN, Brazil
daniel.contadepesquisa@hotmail.com

Eduardo J. C. Cavalcanti
Federal University of Rio Grande do Norte, Department of Mechanical Engineering, 59072-970, Natal/RN, Brazil
educanti@gmail.com

Monica Carvalho
Federal University of Paraíba (UFPB), Department of Renewable Energy Engineering, João Pessoa/Paraíba, Brazil
monica@cear.ufpb.br

Abstract. *The growth in the number of vehicles circulating has led to a greater demand for fossil fuels and consequently, a proportional increase in the emissions of polluting gases. This work presents exergy and exergoenvironmental analyses of a flex-fueled four-stroke spark ignition engine, powered with gasoline-ethanol mixtures (25%, 50%, 75% ethanol by volume). The analyses are developed with experimental results obtained from the engine operated at wide-open throttle conditions, and fixed engine speed (2000 rpm). A Life Cycle Assessment is carried out to quantify the environmental impacts associated with equipment and fuel, employing the Eco-indicator 99 method. The environmental impacts of gasoline and ethanol are 264mPt/kg and 214 mPt/kg, respectively. Pollutants emitted during combustion are measured and included in the environmental assessment (nitrogen oxides, carbon monoxide and dioxide). The fuel blend with 75% ethanol presented the highest exergy efficiency. The effects of the environmental impact rate of pollutant formation and exergy efficiency were significantly higher than the environmental impact rate of fuel. The lowest specific environmental impact of product (shaft power) is 34.48 mPt/MJ, obtained with the fuel blend with 75% ethanol. The combined evaluation of the exergoenvironmental factor and relative difference of environmental impact indicated the optimization priorities and where improvements should be directed.*

Keywords: *Exergoenvironmental Analysis, SPECO, Life Cycle Assessment, Spark-ignition Engine, Gasoline-Ethanol*

1. INTRODUCTION

The internal combustion engine (ICE) was created in 1860, with 4.5 kW and a thermal efficiency of only 5% (Pulkrabek 2004). ICE are the main propulsion systems in road transport (Serrano et al., 2019) and estimates indicate that by 2025 there will be more than 1.5 billion vehicles, with 2 billion vehicles estimated by 2040 (Gis, 2019). In Brazil, gasoline is one of the main fossil fuels employed, and accounts for almost a third of the fuel consumed in the transportation sector, according to the Energy Research Organization (EPE, 2018). The ever-increasing vehicle fleet leads to a higher demand and depletion of fossil fuels, and to an increase the emission of pollutants. Considering global emissions, vehicles are responsible for 20% of carbon dioxide (CO_2) and 70% of carbon monoxide (CO) emissions, in addition to hydrocarbons (HC) and nitrogen oxides (NOx) (Roso et al., 2019). Due to the growing concerns related to the cleaner production of energy, strategies aimed at mitigating and minimizing environmental impacts are essential.

One of the alternatives studied to reduce the emissions of ICE is the use of alternative fuels: ethanol has been a promising candidate, mainly because it is a renewable fuel and can be easily mixed with gasoline (Mourad and Mahmoud, 2019). Several studies have been carried out to analyze engine performance and emissions: Melo et al., (2012) tested a spark-ignition (SI) dual fuel engine with different blends of regular Brazilian gasoline (25% ethanol by volume) and ethanol, and the progressive addition of ethanol resulted in lower CO and HC emissions but increased CO_2 emissions. Al-Hasan (2003) investigated the performance and emissions of a SI engine powered by unleaded gasoline-ethanol mixtures with variable engine speeds (1000 to 4000 rpm), and obtained that the gasoline mixture with 20% ethanol by volume and 3000 rpm resulted in lower emissions and higher performance. Yuan et al., (2019) compared the emissions of the engine running on pure gasoline (E0), with 10% ethanol (E10) and with 27% ethanol (E27), and verified E27 decreased the emissions of particulate matter (PM) and CO. Yanju et al., (2008) operated a 3-cylinder SI engine at full load, with various fractions of methanol (10%, 15%, 20%, 25%, and 30%) in gasoline, and observed that although an increase in methanol resulted in a decrease in torque and power, there was an increase in thermal efficiency. Most studies focus on different fuel mixtures, and compare the atmospheric pollution produced. However, the relationship between the energy produced and environmental damage is not considered, nor does the environmental damage include the production of fuels and of the engine.

In this sense, the exergoenvironmental analysis (Meyer et al., 2009) combines exergy analysis with the Life Cycle Assessment (LCA) methodology to quantify the environmental damage associated with manufacturing the engine and producing the fuels, and helps identify where the environmental impacts are produced and how these are distributed throughout the system. The LCA is a state-of-the-art methodology, internationally consolidated, that quantifies the potential environmental impacts associated with a process or component (Hamut, Dincer, and Naterer, 2014). Exergy analysis is based on the Second Law of Thermodynamics (SLT), which leads to a more meaningful evaluation and comparison of energy conversion systems. Exergy analysis also helps improve and optimize processes and systems, as it provides a measure of efficiency that is closer to reality, taking into consideration the quality of energy, and identifies thermodynamic losses (Dincer and Ratlamwala, 2013). Unlike energy, exergy is not conserved, and the destruction of exergy is one of the main reasons for the low efficiency of ICE (Hoseinpour et al., 2017). Exergoenvironmental assessments can therefore identify the main sources of environmental impacts in energy conversion systems and how these are allocated to internal flows and products, guiding the decision-making process towards environmental sustainability.

Several energy conversion systems have been the focus of exergoenvironmental assessments, especially electricity generation schemes from different energy sources. Meyer et al., (2009) presented a study case to demonstrate the methodology, which was a biomass-based (wood chips) thermochemical system for the production of electricity. Other resources have benefitted from exergoenvironmental analyses, such as eucalyptus biomass (Cavalcanti, Carvalho, and Azevedo, 2019), coal (Rocha and Silva, 2019), solid urban waste (Aghbashlo et al., 2019), and even different diesel-biodiesel blends (Cavalcanti, Carvalho, and Ochoa, 2019).

This work presents exergy and exergoenvironmental analyses of a flex-fueled four-stroke spark ignition engine, powered with gasoline-ethanol mixtures (25%, 50%, 75% ethanol by volume). The analyses are developed with experimental results obtained from the engine operated at wide-open throttle conditions, and fixed engine speed (2000 rpm). Emissions are measured and taken into account in the analysis, along with the environmental impacts associated with manufacturing the engine and producing the fuel, yielding specific environmental impacts (per unit of exergy). LCAs were developed for gasoline and ethanol to assess the environmental impacts. The main contribution of the study presented herein is to verify the behavior of the specific environmental impact associated with the production of power by the ICE, as the proportion of ethanol is increased in the fuel mixtures.

2. MATERIALS AND METHODS

A four cylinder (4C) flex-fuel spark ignition (SI) engine was analyzed on a dynamometer bench test, according to Carvalho (2011). Table 1 shows the specifications of the engine. The mixtures of fuels used were Gasohol E25 (25% anhydrous ethanol, by volume, in gasoline), gasohol E50 mixture (50% anhydrous ethanol, by volume, in gasoline), and gasohol E75 mixture (75% anhydrous ethanol, by volume, in gasoline). Table 2 shows the properties of pure gasoline and ethanol.

Table 1. Engine specifications (Carvalho, 2011).

Engine	GM Powertrain - ECONOFLEX 8V
Cylinders	4 in line
Stroke volume	1389 [cm³]
Compression ration	12.4:1
Max. power – Gasohol / Ethanol	72.8 / 77.2 [kW]
Max. torque – Gasohol / Ethanol	129 / 131 [N.m]
Idle/max. Speed	800 / 6000 [rpm]
Weight	103 [kg]

Table 2. Properties of gasoline and ethanol (Thakur et al., 2017)

Properties	**Gasoline**	**Ethanol**
Chemical Formula	C_5 to C_{12}	C_2H_5OH
Density (kg/m³)	760	785
Molecular weight (kg/kmol)	114.15	46.07
Composition, weight %	-	-
Carbon	87.4	52.2
Hydrogen	12.6	13.1
Oxygen	0	34.7
Adiabatic flame temperature (K)	2270	1920
Higher heating value (MJ/kg)	47.3	29.7
Lower calorific value (MJ/kg)	44.0	26.9
Stoichiometric air fuel ratio	14.2 - 15.1	8.97
Research octane number	95	108
Enthalpy of formation (kJ/kmol)	-	-
Liquid	-259,280	-224,100
Gas	-277,000	-234,600

According to Carvalho (2011), a Schenck model D-210E was utilized (maximum torque capacity 600 Nm and 200 kW power). Fuel consumption was verified by employing the gravimetric method with a 3-decimal resolution scale (Toledo model). A Pitot tube-type anemometer was utilized to measure the flow of intake air, and a K-type temperature sensor was placed in the exhaust pipe to measure the temperature of exhaust gases. The composition of exhaust gases was determined by a TEMPEST 50 - TELEGAN gas analyzer, which provided readings of NOx, CO, CO_2 and O_2. After the engine reached its working temperature, operation data at wide-open throttle (WOT) conditions were obtained for a fixed speed of 2000 rpm. Temperature and pressure of inlet air and fuel were considered as ambient conditions: 25 °C and 101.15 kPa. The pressure of exhaust gases was considered as 101.15 kPa.

2.1 Combustion and Energy Analysis

The chemical formula of gasoline, considering the molecular weight and the mass ratios of carbon and hydrogen as shown in Table 2, is $C_{7.53}H_{13.41}$. Equation (1) describes the combustion of a mixture, based on the molar percentages of gasoline (y_{gas}) and ethanol (y_{eth}) according to their volumetric proportions, with moist atmospheric air.

$$\left[y_{gas}\cdot C_{7.53}H_{13.41}+\ y_{eth}\cdot C_2H_5OH\right]+\lambda\cdot X_{O2}\left[O_2+3.763\cdot N_2+0.092\cdot H_2O_{(g)}+0.0015\cdot CO_2\right]\ \rightarrow \\ \beta_1\cdot CO_2+\beta_2\cdot H_2O+\beta_3\cdot O_2+\beta_4\cdot N_2+\beta_5\cdot NO+\beta_6\cdot CO \tag{1}$$

λ is the theoretical amount of air, X_{O2} is the minimum consumption of oxygen moles per fuel mole for complete combustion in a stoichiometric reaction without excess air, β represents the stoichiometric coefficients of gaseous combustion products evaluated by chemical species balance. The unburned hydrocarbon in exhaust gases was not considered. For each fuel mixture, the molar percentages in eq. (1) are: E25 (0.54 gasoline / 0.46 ethanol), E50 (0.28 gasoline / 0.72 ethanol), and E75 (0.12 gasoline / 0.88 ethanol). The volumetric composition of the moist atmospheric air used in combustion is 0.59% O_2, 77.48% N_2, 1.9% $H_2O_{(g)}$, and 0.03% CO_2.

The control volume considered for the energy analysis encompassed the engine (Figure 1). Steady-state conditions are assumed.

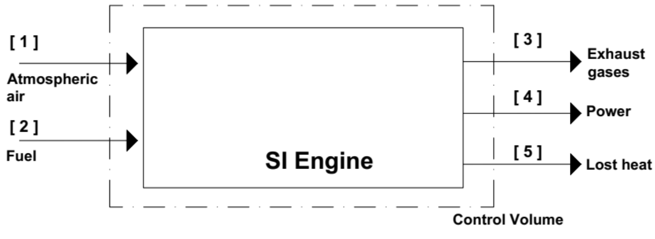

Fig.1. Energy balance in the SI engine.

The First Law of Thermodynamics (FLT) for systems and reagents (Moran et al., 2010) is used to carry out the energy balance, and quantifies the heat losses to the environment, as shown in Eq. (2).

$$\dot{Q}_{CV} + \sum_{R} n_{in}\left(\bar{h}_f^0 + \Delta\bar{h}\right)_{in} = \sum_{P} n_{out}\left(\bar{h}_f^0 + \Delta\bar{h}\right)_{out} + \dot{W}_{CV} \quad (2)$$

Where n is the number of moles of reactants and products in the combustion reaction, $\bar{h}_f^0$ is the enthalpy of formation of each substance, and $\Delta\bar{h}$ is the variation of the formation enthalpy concerning the dead state. Subscripts R and P correspond to the reagent and product, respectively. The formation enthalpy values for gasoline and ethanol follow tab. (2).

2.2 Exergy Analysis

Exergy analysis was based on the *SPecific Exergy COsting* methodology (SPECO), as reported by Lazzaretto and Tsatsaronis (2006). SPECO defines and calculates exergy efficiencies related to exergy costs in thermal systems, based on the records of all additions and removals of exergy flows, establishing a direct link between the definitions of fuel (F) and product (P) for a component. The balance also considers losses of exergy due to heat transfers ($\dot{E}_L$). The exergy balance follows Bejan, Tsatsaronis, and Moran (1995), described by Eq. (3).

$$\dot{E}_F = \dot{E}_P + \dot{E}_L + \dot{E}_D \quad (3)$$

$\dot{E}_D$ is the rate of exergy destruction. The exergy rate of the product ($\dot{E}_P$) will be the axis power measured at point 4 ($\dot{E}_P$ = $\dot{E}_4$). The exergy rate of the ICE fuel ($\dot{E}_F$) is $\dot{E}_1$ + $\dot{E}_2$ - $\dot{E}_3$. The exergy rate of atmospheric air is zero ($\dot{E}_1$ = 0). The exergy rate of the liquid fuel injected into the engine ($\dot{E}_2$) is calculated by multiplying the flow of fuel by its chemical exergy (e^{CH}), calculated according to Appendix-C of Kotas (1985b) for liquid fuels, as shown in Eqs. (4) and (5).

$$e^{CH} = \beta_F \cdot LHV \quad (4)$$

$$\beta_F = 1.0401 + 0.1728 \cdot \left(\frac{H}{C}\right) + 0.0432 \cdot \left(\frac{O}{C}\right) \quad (5)$$

β_F is the ratio of chemical exergy to the net (low) heating value (LHV). C, H, and O are the mass fractions of carbon, hydrogen, and oxygen contained in the fuel, respectively. The accuracy of this expression is estimated to be $\pm$ 0.38 % (Kotas 1985b).

According to Bejan, Tsatsaronis, and Moran (1995), the chemical exergy of a gaseous mixture can be calculated by Eq. (6).

$$e_g^{CH} = \sum_i y_i \cdot e_0^{CH} + R \cdot T_0 \cdot \left(\sum_i y_i \cdot \ln(y_i)\right) \quad (6)$$

Where y_i is the molar fraction of the mixture component; R is the universal gas constant (8.3145 kJ/(kmol.K)), and e_0^{CH} is the standard chemical exergy of each substance according to Appendix-A of Kotas (1985a).

The rate of exergy losses due to heat transfer ($\dot{E}_L$) is calculated according to Eq. (7), following Bejan, Tsatsaronis, and Moran (1995).

$$\dot{E}_L = \dot{Q}_{CV} \cdot \left(1 - \frac{T_0}{T_{surf}}\right) \quad (7)$$

Where $\dot{Q}_{CV}$ is the heat rate; T_0 is the ambient temperature [298.15 K]; and T_{surf} is the surface temperature of the engine, which can also be considered as the thermodynamic average temperature [K].

The exergy efficiency (ε) for the ICE, according to the SPECO methodology (Lazzaretto and Tsatsaronis, 2006), is calculated by Eq. (8).

$$\varepsilon = \frac{\dot{E}_P}{\dot{E}_F} \quad (8)$$

2.3 Life Cycle Assessment (LCA)

LCA is standardized by the International Organization for Standardization (ISO) in its standards ISO 14040 (2006) and ISO 14044 (2006), and according to the European Commission (2019), the LCA methodology provides the best currently available framework for the assessment of potential environmental impacts of products, processes, and systems. LCA enables the assessment of the environmental impacts associated with all the stages of a product (or process), which can encompass raw material extraction and processing, manufacture, distribution, use, maintenance and final disposal. A LCA is constituted by four interrelated steps (Hauschild et al., 2018): definition of scope and goal, overall inventory analysis, impact assessment, and interpretation.

Definition of scope and goal includes the definition of the functional unit, to which all inputs and outputs of the study object are related to. The next step builds an inventory with all mass and energy flows associated with the functional unit. The third step is when an environmental impact assessment method is selected, which can express the environmental impacts in different metrics. Interpretation of results includes the drawing of conclusions and recommendations.

The environmental impact assessment method selected herein was the Eco-indicator 99 (EI99) (Goedkoop, Effting, and Collignon 2000), which includes damages to human health, ecosystem quality and the use of resources. EI99 includes normalization and weighting steps in the LCA, and assigns a single score to each product or process, calculated based on the relative environmental impact. The score is represented in points, in which each point represents the annual environmental load (i.e., overall production/consumption undertakings in the economy) of an average European citizen (Singh et al., 2018).

The environmental impact related to the SI engine was determined from its material composition according to Yang, Wang, and Jiao (2020), and is shown in Tab. 3.

Table 3. Material composition and environmental impacts of the SI engine (construction phase).

Material	**Weight composition (%)**	**Specific impact (mPt/kg)**	**Overall impact (mPt/kg)**
Steel	18.52	86	15.93
Iron	60.60	240	145.43
Aluminum	19.76	780	154.16
Polypropylene	0.75	330	2.46
Rubber	0.37	360	1.34
Total	**100.00**		**319.32**

For the development of the LCA for gasoline and ethanol, software SimaPro v.9.1.0.8 (2020) was utilized, with the Ecoinvent database 3.5 (2018), and EI99 method (Goedkoop, Effting, and Collignon, 2000). Table 4 shows the composition and environmental impacts of the gasoline-ethanol mixtures employed herein. These values do not include combustion.

Table 4. Composition and environmental impacts of the gasoline-ethanol mixtures.

Fuel	**Overall impact (Pt/kg)**
Gasoline	0.264
Gasoline E25	0.251
Gasoline E50	0.239
Gasoline E75	0.226
Ethanol	0.214

The process for gasoline considered the production of unleaded gasoline at the oil refinery. Operation of storage tanks and refinery facilities are considered, along with transportation of product from the refinery to the end user. Operation of storage tanks and petrol stations are included, as well as emissions from evaporation and treatment of effluents.

For ethanol, the process is modelled with ethanol production from sugarcane[1] in Brazil. This dataset includes the transport of sugarcane to the sugar refinery and the processing of sugarcane to ethanol (95% w/w), bagasse (79% dry matter, excess), and vinasse. System boundary is at the sugar refinery. Treatment of waste effluents is not included (most wastewater is spread over the fields nearby).

2.4 Exergoenvironmental Assessment

The methodology was developed by Meyer et al. (2009), who indicated that an understanding of the formation of environmental impacts is essential to improve the ecological performance of energy conversion systems. The method identifies the sources of environmental impact and tracks the formation of pollutants throughout the system.

The exergoenvironmental analysis consists of three steps: i) Exergy analysis of the energy conversion system; ii) LCA of the energy conversion equipment and of all associated input and output energy streams, and iii) Allocation of environmental information obtained via LCA to all exergy flows of the system.

The exergoenvironmental assessment allocates environmental impacts to the respective k-th exergy flows (Meyer et al. 2009), according to Eq. (9).

$$\dot{B}_K = b_K \cdot \dot{E}_K \tag{9}$$

$\dot{B}_k$ is the rate of environmental impact, in points per unit of time (mPt/s); b_k is the specific environmental impact (per unit of exergy) of the same flow (mPt/GJ); $\dot{E}_k$ is the exergy rate of the corresponding flow.

Equation (10) describes the exergoenvironmental balance for the SI engine, which encompasses the specific environmental impacts of the input associated with the respective exergy flows, plus the environmental impact rate related to the engine ($\dot{Y}$). This is equal to the sum of the specific environmental impacts of the associated output to all respective flows of exergy (Bejan, Tsatsaronis, and Moran, 1995).

$$\dot{B}_F + \dot{Y} + \dot{B}^{PF} = \dot{B}_P + \dot{B}_L \tag{10}$$

$\dot{B}_F$ is the environmental impact rate of the fuel for the component (mPt/s), $\dot{B}^{PF}$ is the environmental impact rate associated with pollutant formation (mPt/s), $\dot{B}_P$ is the environmental impact rate of the product (mPt/s), $\dot{B}_L$ is the environmental impact rate of exergy losses (mPt/s), and $\dot{Y}$ is the environmental impact rate related to the engine, considering a lifetime of 20 years with 8000 operation hours per year.

The environmental impact rate associated with the formation of pollutants ($\dot{B}^{PF}$) is expressed by Eq. (11) (Cavalcanti, Carvalho, and Azevedo, 2019).

$$\dot{B}^{PF} = \sum b_i^{PF} \cdot (\dot{m}_{i,out} - \dot{m}_{i,in}) \tag{11}$$

$\dot{m}_{i,out}$ and $\dot{m}_{i,in}$ are the mass flows of pollutants associated with the inputs and outputs of the engine, respectively; b_i^{PF} is the specific environmental impact (per unit mass) of the corresponding type of pollutant. According to Goedkoop and Spriensma, (2001), the environmental impacts for each pollutant produced by the combustion considered in Eq. (1) are 8.36 mPt/kg for CO, 5.45 mPt/kg for CO_2, and 4217.74 mPt/kg for NO.

The exergoenvironmental equations for the environmental impact rates are shown in Tab. 5., along with corresponding auxiliary equations (Lazzaretto and Tsatsaronis, 2006), where the Fuel (F) principle is applied.

[1] The dataset includes the inputs of mineral fertilizers and industrial residues (as fertilizers and pesticides). There is no input of seedlings in the dataset. All machine operations are included, with infrastructure for machinery shelter and maintenance. Most agricultural operations are manual, and the inventory represent Brazilian averages. Direct field emissions are included, with important regionalizations added. Transportation of products inside the farm is considered.

Table 5. Exergoenvironmental equations

Environmental Impact Rates (mPt / s)	**Exergoenvironmental Equations**	**Auxiliary Equations**
Product ($\dot{B}_P$)	$b_4 \cdot \dot{E}_4$	
Fuel ($\dot{B}_F$)	$b_1 \cdot \dot{E}_1 + b_2 \cdot \dot{E}_2 - b_3 \cdot \dot{E}_3$	$b_1 = 0; b_2 = b_3$
Loss of Exergy ($\dot{B}_L$)	$b_F \cdot \dot{E}_L$	
Destruction of Exergy ($\dot{B}_D$)	$b_F \cdot \dot{E}_D$	

The average environmental impact per exergy unit of fuel is evaluated using the fuel and exhaust gases flows according to Lazzaretto and Tsatsaronis. 2006, as shown in Eq. (12).

$$b_F = \left(\frac{b_1.\dot{E}_1 + b_2.\dot{E}_2 - b_3.\dot{E}_3}{\dot{E}_1 + \dot{E}_2 - \dot{E}_3}\right) \tag{12}$$

Where the exergy rate $\dot{E}_1$ is null.

According to Meyer et al. (2009), the environmental impact per unit of exergy of the product (shaft power produced by the engine) considers the reallocation of environmental losses associated with the rate of heat losses. The total environmental impact rate ($\dot{B}_{Tot}$) is the sum of the environmental impacts (Meyer et al., 2009), expressed by Eq. (13).

$$\dot{B}_{Tot} = \dot{Y} + \dot{B}^{PF} + \dot{B}_D + \dot{B}_L \tag{13}$$

$\dot{Y}$, $\dot{B}^{PF}$, $\dot{B}_D$, $\dot{B}_L$ are the rates of environmental impacts related to the component itself, formation of pollutants, destruction of exergy, and exergy losses associated to heat transfer, respectively.

The relative difference (r_b) takes into account the average environmental impacts rate per exergy unit of the product (b_P) and fuel (b_F) of a component, and indicates the potential for reducing the environmental impact with less effort. r_b represents the environmental quality of a component, as given by Eq. (14) (Meyer et al., 2009):

$$r_b = \left(\frac{b_P - b_F}{b_F}\right) \tag{14}$$

The exergoenvironmental factor (f_b) assesses the relative contribution of the environmental impact related to the component ($\dot{Y}$) concerning the sum of the environmental impacts (Meyer et al. 2009) and the formation of pollutants, as presented by Eq. (15) (Cavalcanti, Carvalho, and Ochoa 2019).

$$f_b = \left(\frac{\dot{Y} + \dot{B}^{PF}}{\dot{B}_{Tot}}\right) \tag{15}$$

If f_b is higher than 0.7 the environmental impact related to the component is dominant, if less than 0.3 the environmental impact due to the destruction of exergy is dominant.

3. RESULTS AND DISCUSSION

Exergy and exergoenvironmental assessments are developed for a flex-fuel SI engine powered with gasoline-ethanol mixtures (25%, 50%, 75% ethanol by volume). Wide-open throttle (WOT) conditions and fixed engine speed (2000 rpm) were considered. Emissions were measured and taken into account in the analysis.

3.1 Combustion and Exergy Analysis

The stoichiometric air-fuel ratio (mass base) was calculated for the fuel mixtures E25, E50, and E75 resulting in 13.09, 11.72, and 10.38, respectively. With the increase in the percentage of ethanol, the stoichiometric requirements are reduced, as ethanol is an oxygenated fuel and already has oxygen molecules in its composition.

Table 6 shows the data used in the models and the results of combustion balance. The mass fuel flow ($\dot{m}_F$), mass airflow ($\dot{m}_{air}$), and exhaust gas temperature (T_g) were collected from Carvalho (2011). The pollutants and lambda factor (λ) were evaluated using the stoichiometric balance of the combustion equation, eq. (1).

Table 6. Measured data and combustion analysis

FUEL	$\dot{m}_F$ [g/s]	$\dot{m}_{air}$ [g/s]	T_g [°C]	NO_x [g/kg FUEL]	CO [g/kg FUEL]	CO_2 [g/kg FUEL]	λ
E25	1.583	23.44	717.00	3.57	1.82	179.30	1.131
E50	1.767	23.56	681.00	3.42	2.35	174.40	1.138
E75	1.900	21.96	677.00	3.00	2.58	173.80	1.113

λ is the ratio between the actual air-fuel ratio (measured experimentally) and the stoichiometric air-fuel ratio. The engine operating on a higher ethanol content increases its mass flow. Consequently, with the reduction of gasoline in volume, the temperature of the exhaust gases is lower. CO_2 emissions reduce from 179.30 to 173.80 grams of CO_2 per kg of fuel burned, and the emission of NO_x is also reduced, from 3.57 to 3.00 grams of NO_x per kg of fuel burned. However, the emission of carbon monoxide increases from 1.82 to 2.58 grams of CO per kg of fuel burned.

Table 7 shows the results of the exergy analysis for each fuel (E25, E50, E75), showing the related exergy rates: fuel ($\dot{E}_2$), exhaust gases ($\dot{E}_3$), losses ($\dot{E}_5$) due to heat transfer, and shaft power ($\dot{E}_4$). These flows have been aforedescribed in Figure 1. Following the SPECO methodology, the results of the product ($\dot{E}_P$) and fuel ($\dot{E}_F$) for the engine are presented, in addition to the exergy rate destroyed ($\dot{E}_D$), evaluated by equation 3.

Table 7. Exergy analysis results

FUEL	$\dot{E}_2$ [kW]	$\dot{E}_3$ [kW]	$\dot{E}_4$ [kW]	$\dot{E}_5$ [kW]	$\dot{E}_P$ [kW]	$\dot{E}_F$ [kW]	$\dot{E}_D$ [kW]
E25	67.32	12.44	19.9	16.21	19.9	54.88	18.77
E50	67.58	11.97	20.21	16.84	20.21	55.61	18.56
E75	64.71	11.4	19.69	16.53	19.69	53.31	17.09

The fuel exergy rate ($\dot{E}_F$) of the engine combines the exergy rate of point 2 (inlet of gasoline-ethanol mixture) minus the exergy rate of the exhaust gases at point 3, according to the SPECO methodology. The exergy rate at point 2 only presents chemical exergy, calculated by eq. (4), by which the results were 42.52 MJ/kg, 38.25 MJ/kg, and 34.05 MJ/kg for the E25, E50, and E75 blends, respectively. The higher the ethanol content, the lower the chemical exergy of the fuel, which justifies the reduction of the fuel exergy rate ($\dot{E}_2$). The exergy rate of the exhaust gases ($\dot{E}_3$) depends on the mass flow of gases and its temperature at the outlet. With the increase in ethanol content, there is a reduction in the temperature of the gases, Table (6), resulting in a reduction of the exergy rate of gases ($\dot{E}_3$). The exergy rate of the product ($\dot{E}_P$) represents the shaft power produced by the engine at point 4, according to fig. (1). The rate of exergy destroyed ($\dot{E}_D$) is calculated by the exergy balance, eq. (3), which presents a slight reduction as concentration increases. The fuel exergy rate ($\dot{E}_F$) is a result of the chemical exergy of the fuel, and its mass flow. As the ethanol content increases, the chemical exergy of the fuel reduces, and its mass flow increases. The fuel exergy rate ($\dot{E}_F$) increases to E50 and then reduces. The rate of exergy losses associated with heat transfer ($\dot{E}_5$) is a function of the rate of heat loss and of the surface temperature of the engine, according to eq. (7). The increase in ethanol content does not cause significant variations.

The exergy efficiency is the ratio between the exergy rates of the product ($\dot{E}_P$) and fuel ($\dot{E}_F$), and Fig. 2 shows how the exergy efficiency changes with the addition of ethanol to the fuel mixture.

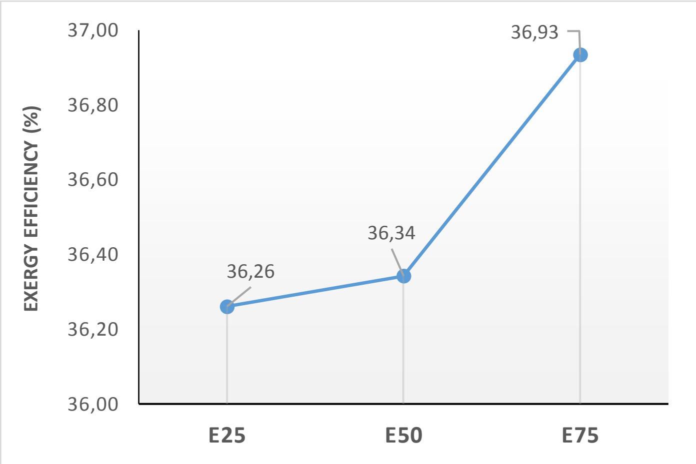

Fig. 2. Ethanol content *vs.* exergy efficiency.

The exergy efficiency of the engine increases along with the ethanol content in the mixture, from 36.26% (E25) to 36.93% (E75). A similar result was observed by Rufino et al. (2019), in which the exergy efficiency of the engine was tested for rotations from 1000 to 5000 rpm. The exergy efficiency of the engine was higher for ethanol than for gasoline.

3.2 Exergoenvironmental Analysis

Table 8 shows the results of the exergoenvironmental balance calculated by eq. (10). The values of the specific environmental impacts were calculated: fuel (b2), exhaust gases (b3), shaft power (b4), and exergy losses (b5). The environmental impact rates of the product ($\dot{B}_P$) and fuel ($\dot{B}_F$) were calculated according to the SPECO method, described by Meyer et al. (2009), and shown in tab. (5). Environmental impact rates related to exergy losses ($\dot{B}_L$), exergy destruction ($\dot{B}_D$), and associated with pollutant formation ($\dot{B}^{PF}$) are also shown in Table 8.

Table 8. Exergoenvironmental results

FUEL	b_2 [mPt/MJ]	b_3 [mPt/MJ]	b_4 [mPt/MJ]	b_5 [mPt/MJ]	$\dot{B}_F$ [mPt/s]	$\dot{B}_P$ [mPt/s]	$\dot{B}_L$ [mPt/s]	$\dot{B}_D$ [mPt/s]	$\dot{B}^{PF}$ [mPt/s]
E25	5.908	5.908	31.670	5.908	0.324	0.630	0.096	0.111	0.402
E50	6.237	6.237	31.230	6.237	0.347	0.631	0.105	0.116	0.389
E75	6.643	6.643	28.900	6.643	0.354	0.569	0.110	0.114	0.325

The environmental impact rate related to engine production ($\dot{Y}$) has a constant value of 0.206 mPt/h, considering the environmental impact of the material composition (table 3) and the weight of the engine, 103 kg.

The specific environmental impact of the fuel (b2) becomes higher as the ethanol content increases. Although gasoline has a higher environmental impact per unit mass (264 mPt/kg) than ethanol (214 mPt/kg), the increase in fuel flow generates a higher environmental impact of fuel (b2) according to eq. (2). It must be highlighted that this environmental impact is from “cradle to gate”, and does not include combustion (there is a high contribution to the environmental impacts due to the formation of pollutants during combustion). When applying the exergy flow to the respective point, the environmental impact rates for each fuel is 1431.82 mPt/h, 1517.39 mPt/h, and 1547.53 mPt/h for the E25, E50, and E75 blends, respectively.

The specific environmental impact of the exhaust gases (b3) and exergy losses (b5) are equal to that of the fuel (b2), according to the FUEL-method approach within the SPECO methodology.

The environmental impact rates, related to the exergy flows, for each fuel mixture (E25, E50, and E75), are respectively: for exhaust gases ($\dot{B}_3$) 264.58 mPt/h, 268.76 mPt/h, and 272.63 mPt/h, and for exergy losses ($\dot{B}_L$) 344.77 mPt/h, 378.11 mPt/h, and 395.31 mPt/h. The rates of environmental impact related to the exhaust gases ($\dot{B}_3$) and exergy losses ($\dot{B}_L$) increase with higher ethanol contents, due to the increase in the specific environmental impact of the fuel (b2) due to its higher flow.

Table 8 also shows the average environmental impact rate per exergy unit of product – power - ($\dot{B}_P$) and fuel ($\dot{B}_F$) of the engine. As the ethanol content increases, there is a reduction in the average environmental impact rate per exergy unit of power ($\dot{B}_P$), due to a reduction in the specific environmental impact of the power produced (b4), because of the exergoenvironmental balance in eq. (10). The rate of environmental impact related to the destruction of exergy ($\dot{B}_D$), also shown in table 8, does not present significant variations, due to the increase in the specific environmental impact of the fuel (b2). There is a reduction in the rate of destroyed exergy ($\dot{E}_D$) with the increase of ethanol content in the mixture. With the increase in ethanol content, there is a reduction in the environmental impact rate related to the formation of pollutants ($\dot{B}^{PF}$), calculated by eq. (11).

Figure 3 shows the environmental impact rates of the fuel ($\dot{B}_2$) and pollutant formation ($\dot{B}^{PF}$), considering different gasoline-ethanol mixtures.

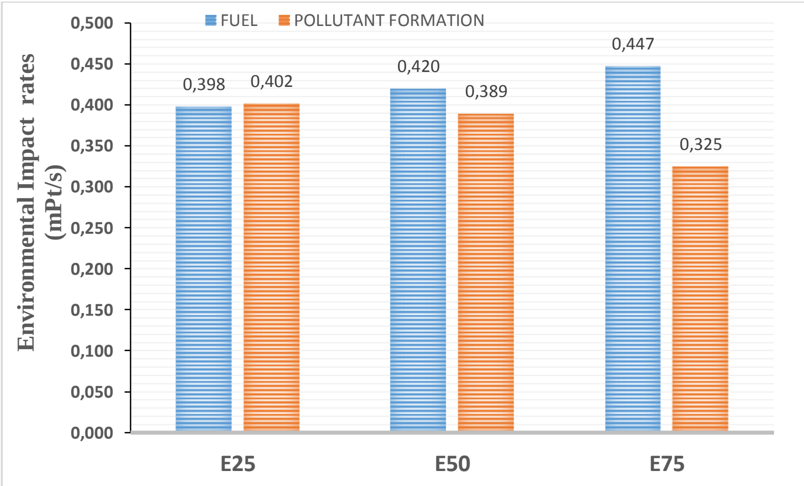

Fig. 3. Variation of environmental impact rates with ethanol content.

As shown in Fig. (3), even with the increase in the environmental impact rate of the fuel ($\dot{B}_2$) entering the engine, the lower environmental impact rates are produced due to the reduction in the mass flow of exhaust gases. The mass flow of each polluting gas is multiplied by the environmental impact per unit of mass of each gas (8.36 mPt/kg for CO, 5.45 mPt/kg for CO_2, and 4217.74 mPt/kg for NOx). Melo et al. (2012) tested a SI engine with different mixtures of Brazilian gasoline (25% ethanol by volume) and ethanol, and the progressive addition of ethanol resulted in lower CO and HC emissions, however increased emissions of CO_2.

Figure (4.a) shows the measured emissions (CO, NOx) and the emissions calculated by the combustion mass balance (Table (4)). Moreover, figure (4.b) depicts the participation of each polluting gas in the environmental impact rate of pollutant formation ($\dot{B}^{PF}$).

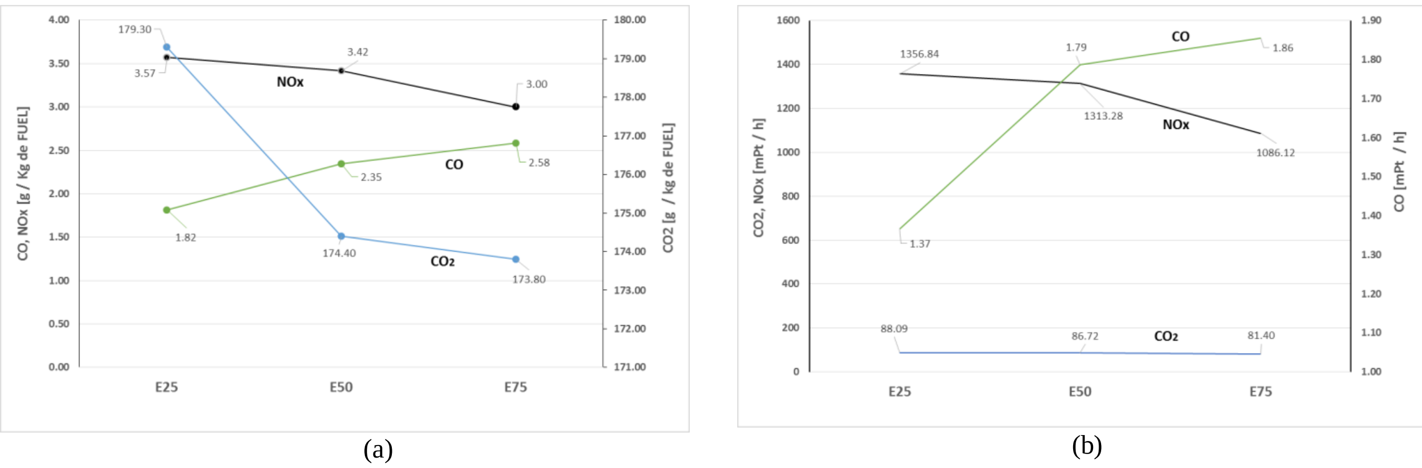

Fig. 4. (a) Pollutant gas emissions; (b) environmental impact rate for each polluting gas.

In figure (4.a), the left y-axis represents the emissions of CO and NOx, and the right y-axis shows the emissions of CO_2. As the ethanol content increases, there is a reduction in CO_2 and NOx emissions and an increase in CO emissions, as occurred with Melo et al. (2012).

Figure (4.b) follows the same axis nomenclature, and with the increase in ethanol content, an increase in the contribution of CO is verified, from 1.37 mPt/h to 1.86 mPt/h. The environmental impact rate associated with CO_2

decreases from 88.09 mPt/h to 81.40 mPt/h; and the contribution of NOx presents a reduction from 1356.84 mPt/h to 1086.12 mPt/h.

Figure 5 shows the specific environmental impact of the shaft power produced (b_P) as a function of the ethanol content in the fuel.

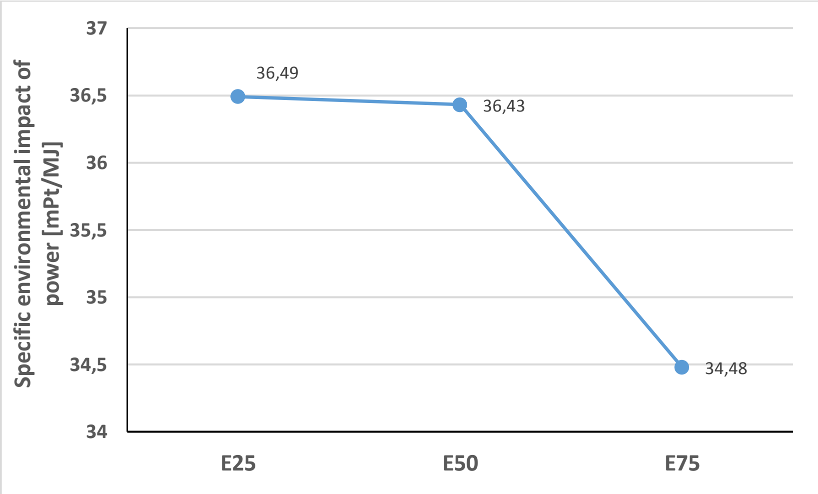

Fig. 5. Specific environmental impact *vs.* ethanol content.

In figure 5, the specific environmental impact rate of produced power (b_P) decreases with an increase in the ethanol content, from 36.49 mPt/MJ to 34.48 mPt/MJ. This reduction follows the increase in exergy efficiency, as seen in fig. (2).

In scientific literature, no similar work was found focusing on Otto cycle internal combustion (IC) engines. Cavalcanti, Carvalho, and Ochoa (2019) carried out an exergoenvironmental analysis for diesel-biodiesel blends in a direct injection engine at variable loads, and verified that higher biodiesel contents improved the efficiency of the engine, and lowered the specific environmental impact of electricity.

Figure 6 shows the exergoenvironmental factor (f_b) on the primary y-axis, and the relative difference of environmental impact (r_b) on the secondary y-axis.

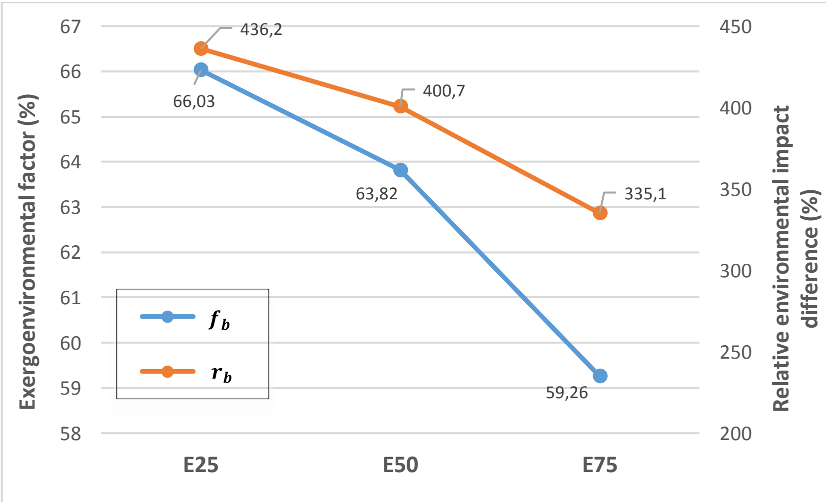

Fig. 6. Exergoenvironmental factor and relative difference of environmental impact *vs.* ethanol content.

The r_b values decrease from 436.2% to 335.1%, when the ethanol content increases. According to Meyer et al. (2009), r_b represents the environmental quality of a component, and thus the addition of ethanol improves the engine's environmental quality. The value of f_b decreases with the increase in ethanol content, indicating that the relative contribution of pollutant formation to the overall value of environmental impacts is decreasing, as the environmental impact relative to the engine is constant.

4. CONCLUSIONS

Exergy and exergoenvironmental analyses were developed for a four-stroke spark ignition engine with maximum power of 77.2 kW. The engine is fueled with gasoline-ethanol mixtures (25%, 50%, 75% ethanol by volume), and operates at a constant speed of 2000 rpm.

The mixture with 25% of ethanol presented the higher NOx and CO_2 emissions. The mixture with 75% ethanol presented the highest fuel consumption rate and CO emissions.

The highest exergy efficiency (36.93%) was reached with the 75% ethanol blend. The highest specific environmental impact related to fuel (b2) was 6.643 mPt/MJ for the 75% ethanol blend, followed by the 50% ethanol blend with 6.237 mPt/MJ. Although the environmental impact associated with ethanol is lower than gasoline (214 vs. 264 mPt/kg, which does not include combustion).

The highest environmental impact rate associated with the formation of pollutants was obtained for 25% ethanol blend.

The lowest specific environmental impact of product (shaft power) was achieved for the 75% ethanol blend. This condition presented the best environmental impact performance. When the 75% ethanol fuel is employed, the lowest exergoenvironmental factor (f_b) and higher relative difference of environmental impact (r_b) were obtained, indicating that there is potential for improvements.

Further research can focus on the environmental performance at different speeds.

5. ACKNOWLEDGEMENTS

The authors wish to acknowledge the support of the National Council for Scientific and Technological Development (CNPq, Brazil) Research Productivity grant nº 307394/2018-2.

6. REFERENCES

Aghbashlo, M., Tabatabaei, M., Soltanian, S., Ghanavati, H., 2019. “Biopower and Biofertilizer Production from Organic Municipal Solid Waste: An Exergoenvironmental Analysis.” *Renewable Energy,* Vol. 143, pp. 64–76.

Al-Hasan, M., 2003. “Effect of Ethanol–Unleaded Gasoline Blends on Engine Performance and Exhaust Emission.” *Energy Conversion and* Managementm, Vol. 44, No.9, pp. 1547–61.

Bejan, A., Tsatsaronis, G., Moran, M. J., 1995. *Thermal Design and Optimization*. John Wiley & Sons.

Carvalho, M. A. S, 2011. “Evaluation of an Otta-Cycle Internal Cmbustion Engine Using Different Fuels" (Thesis in Portuguese).” https://repositorio.ufba.br/ri/handle/ri/18744 - UFBA/Brazil.

Cavalcanti, E. J. C., Carvalho, M., Azevedo, J. B., 2019. “Exergoenvironmental Results of a Eucalyptus Biomass-Fired Power Plant.” *Energy*, Vol. 189, pp. 116188.

Cavalcanti, E. J. C., Carvalho, M., Ochoa, A. A. V., 2019. “Exergoeconomic and Exergoenvironmental Comparison of Diesel-Biodiesel Blends in a Direct Injection Engine at Variable Loads.” *Energy Conversion and Management,* Vol. 183, pp. 450–461.

Dincer, I., Ratlamwala, T. A. H., 2013. “Importance of Exergy for Analysis, Improvement, Design, and Assessment.” *WIREs Energy and Environment*, Vol. 2, No. 3, pp. 335–349.

Ecoinvent, 2018, “The ecoinvent database 3.5”, Available at: <http://www.ecoinvent.org/>, Accessed 26 jul 2020.

EPE. 2018. “Summary Report - Year 2017 - EPE.” In *Energy Research Office*. Rio de Janeiro. http://www.epe.gov.br/en.

EUROPEAN COMMISSION European Platform on Life Cycle Assessment (LCA), 2019. https://ec.europa.eu/environment/ipp/lca.htm. Accessed May 06, 2020.

Gis, M. 2019. “Assessment of Exhaust Emissions from Vehicles in Real Traffic Conditions.” *IOP Conference Series: Earth and Environmental Science*, Vol. 214, pp. 012035.

Goedkoop, M, Spriensma, R., 2001. “The Eco-Indicador 99: A Damage Oriented Method for Life Cycle Impact Assessment e Methodology Report. Netherlands: Pre Consultants” 3rd. http://www.pre-sustainability.com/download/misc/EI99_methodology_v3.pdf.

Goedkoop, M., Effting, S., Collignon, M., 2000. “The Eco-Indicator 99: A Damage Oriented Method for Life-Cycle Impact Assessment: Manual for Designers.” PRé Consultants. http://www.pre-sustainability.com/download/manuals/EI99_Manual.pdf.

Hauschild, M.K., Rosenbaum, R. K., Olsen, S. I. (Eds.). Life Cycle Assessment, Springer, 2018.

ISO 14040. Environmental management - Life cycle assessment - Principles and framework. International Organization for Standardization (ISO), Geneva, 2006.

ISO 14044. Environmental management - Life cycle assessment - Requirements and guidelines. International Organization for Standardization (ISO), Geneva, 2006.

Hamut, H. S., Dincer, I., Naterer, G. F., 2014. “Exergoenvironmental Analysis of Hybrid Electric Vehicle Thermal Management Systems.” *Journal of Cleaner Production*, Vol. 67, pp. 187–196.

Hoseinpour, M., Sadrnia, H., Tabasizadeh, M., Ghobadian, B., 2017. “Energy and Exergy Analyses of a Diesel Engine Fueled with Diesel, Biodiesel-Diesel Blend and Gasoline Fumigation.” *Energy*, Vol. 141, pp. 2408–2420.

Kotas, T J. 1985a. “Appendix A - Chemical Exergy and Enthalpy of Devaluation.” In *The Exergy Method of Thermal Plant Analysis*, edited by T J Kotas, 236–62. Butterworth-Heinemann. https://doi.org/10.1016/B978-0-408-01350-5.50014-3.

———. 1985b. “Appendix C - Chemical Exergy of Industrial Fuels.” *The Exergy Method of Thermal Plant Analysis*, 267–69. https://doi.org/10.1016/b978-0-408-01350-5.50016-7.

Lazzaretto, A., Tsatsaronis, G., 2006. “SPECO: A Systematic and General Methodology for Calculating Efficiencies and Costs in Thermal Systems.” *Energy*, Vol. 31, No. 8, pp 1257–1289.

Melo, T. C. C., Machado, G. B., Belchior, C. R., Colaço, M. J., Barros, J. E., Oliveira, E. J., Oliveira, D. G., 2012. "Hydrous ethanol–gasoline blends–Combustion and emission investigations on a Flex-Fuel engine". *Fuel*, Vol. 97, pp. 796-804.

Meyer, L., Tsatsaronis, G., Buchgeister, J., Schebek, L., 2009. “Exergoenvironmental Analysis for Evaluation of the Environmental Impact of Energy Conversion Systems.” *Energy*, Vol. 34, No. 1, pp. 75–89.

Moran, M. J., Shapiro, H. N., Boettner, D. D., Bailey, M. B. 2010. *Fundamentals of Engineering Thermodynamics*. John Wiley & Sons.

Mourad, M., Mahmoud, K., 2019. “Investigation into SI Engine Performance Characteristics and Emissions Fuelled with Ethanol/Butanol-Gasoline Blends.” *Renewable Energy*, Vol. 143, pp. 762–771.

Pulkrabek, W. W., 2004. *Engineering Fundamentals of the Internal Combustion Engine*. 2nd Ed. ASME.

Rocha, D. H. D., Silva, R. J., 2019. “Exergoenvironmental Analysis of a Ultra-Supercritical Coal-Fired Power Plant.” *Journal of Cleaner Production*, Vol. 231, pp 671–682.

Roso, V. R., Santos, N. D. S. A., Alvarez, C. E. C., Rodrigues Filho, F. A., Pujatti, F. J. P., & Valle, R. M., 2019. "Effects of mixture enleanment in combustion and emission parameters using a flex-fuel engine with ethanol and gasoline". *Applied Thermal Engineering*, Vol. 153, pp. 463-472.

Simapro, 2020, “Software SimaPro v.9.1.0.8”, Available at: <www.simapro.nl>, Accessed 26 jul 2020.

Singh, V., Dincer, I., Rosen, M. A., 2018. Life cycle assessment of ammonia production methods. In Exergetic, Energetic and Environmental Dimensions (pp. 935-959). Academic Press.

Serrano, J. R., Novella, R., Piqueras, P., 2019. "Why the development of internal combustion engines is still necessary to fight against global climate change from the perspective of transportation". *Appl. Sci.*, Vol. 9, No. 21, pp. 4597.

Thakur, A. K., Kaviti, A. K., Mehra, R. Mer, K. K. S., 2017. “Progress in Performance Analysis of Ethanol-Gasoline Blends on SI Engine.” *Renewable and Sustainable Energy Reviews*, Vol. 69, pp 324–340.

Yang, Z., Wang, B., Jiao, K., 2020. “Life Cycle Assessment of Fuel Cell, Electric and Internal Combustion Engine Vehicles under Different Fuel Scenarios and Driving Mileages in China.” *Energy*, Vol. 198, pp. 117365.

Yanju, W., Shenghua, L., Hongsong, L., Rui, Y., Jie, L., Ying, W., 2008. “Effects of Methanol/Gasoline Blends on a Spark Ignition Engine Performance and Emissions.” *Energy and Fuels*, Vol. 22, No. 2, pp. 1254–1259.

Yuan, W., Frey, H. C., Wei, T., Rastogi, N., VanderGriend, S., Miller, D., Mattison, L., 2019. “Comparison of Real-World Vehicle Fuel Use and Tailpipe Emissions for Gasoline-Ethanol Fuel Blends.” *Fuel*, Vol. 249, pp. 352–364.

7. RESPONSIBILITY NOTICE

The authors are the only responsible for the printed material included in this paper